Physica E 44 (2012) 1503–1509

Contents lists available at SciVerse ScienceDirect

Physica E

journal homepage: www.elsevier.com/locate/physe

Optimal design of heterostructure tunnel diode with nonlinear current–voltage characteristic

Kelly C. Magruder, A.F.J. Levi *

Department of Electrical Engineering, University of Southern California, Los Angeles, CA 90089-2533, USA

ARTICLE INFO

Article history:
Received 1 December 2011
Accepted 15 March 2012
Available online 29 March 2012

ABSTRACT

Optimal design applied to an $Al_{\xi}Ga_{1-\xi}As$ heterostructure tunnel diode is used to achieve a parametrically defined nonlinear current–voltage characteristic. The design predicts that a significant reduction in spurious frequency components from a switching RF mixer can be realized using a device that is less than 17 nm thick.

1. Introduction

Nonequilibrium electron transport over length scales less than an inelastic electron mean-free-path, λ_{in}, can be sufficiently coherent that the wave nature of the electron plays an important role in determining current flow. In semiconductor nanowires and single-walled carbon nanotubes with characteristic size $\ll \lambda_{in}$ and no scattering in the active region, wave-like electron behavior and dimensional confinement gives rise to linear (ohmic) current–voltage characteristics. In this situation, quantized conductance is $G_n = e^2/2\pi\hbar$ or $(25.8\ \mathrm{k\Omega})^{-1}$ per electron spin. Ohmic resistance greater than $1/G_n$ is not directly accessible via quantized conductance. However, we have previously shown how optimal design and atomic layer precision in fabrication of heterostructure tunnel diodes only a few nm thick may be used to circumvent this limitation and accurately mimic ohmic behavior over a very wide range of resistance values [1]. This is achieved by manipulating low-energy elastic electron scattering and electron transmission resonances in an optimally designed semiconductor heterostructure band-edge potential profile.

Availability of linear current–voltage characteristics in nano-scale devices satisfies only one type of building block for circuits. Nano-scale structures with *nonlinear* characteristics represent a much broader class of circuit element. It is very important to demonstrate that nano-scale devices can access *useful* nonlinear behavior for, among other things, analog processing of electronic signals. This presents special challenges for nano-scale electronic component design. First, the characteristics of the ideal nonlinearity must be identified and, second, a structure with the required behavior must be physically feasible.

In its most general form the design of nano-scale nonlinear electronic circuit elements is a formidable problem. In part, this is because of the vast number of possible nonlinearities, numerous circuit topologies to which they may be applied, the possibility of unstable circuit behavior, and limited device performance imposed by the physics of nonequilibrium electron transport that occurs in necessarily small ($\ll \lambda_{in}$) nano-scale device active regions.

To make progress to the level of proof-of-principle, we focus on a RF mixer because it is a prototypical nonlinear analog signal processing circuit. We show how to quantify the nonlinear device behavior needed to dramatically improve the performance of a RF mixer. We then demonstrate that it is physically possible to capture much of the potential performance gain using an optimally designed $Al_{\xi}Ga_{1-\xi}As$ heterostructure tunnel diode with a nonlinear current–voltage characteristic. The device is designed to operate at room temperature and the active region is less than 17 nm thick.

2. Ideal switching mixer

In a RF receiver the input signal of amplitude V_{RF} and frequency $\omega_{RF} = 2\pi f_{RF}$ is mixed with a local oscillator (LO) signal of amplitude V_{LO} and frequency $\omega_{LO} = 2\pi f_{LO}$ to extract a desired signal from a carrier. The LO is tuned to select an intermediate frequency (IF) of amplitude V_{IF} and frequency $\omega_{IF} = |\omega_{LO} - \omega_{RF}|$. One method of accomplishing this mixing is by using the LO signal to switch the phase of the RF signal [2]. A full-wave rectifier similar to that shown in Fig. 1 may be implemented using either diodes as shown or transistors as switching devices. To illustrate the design concept we adopt the architecture of Fig. 1. In the figure the series resistance of the voltage source is R_S and the output signal, V_{out}, is taken across the load resistance, R_L.

The ideal output of the switching mixer is

$$V_{out}(t) = \frac{R_L}{R_S + R_L} |V_{in}(t)|, \tag{1}$$

* Corresponding author. Tel.: +1 213 740 7318.
E-mail address: alevi@usc.edu (A.F.J. Levi).

1386-9477/$ - see front matter © 2012 Elsevier B.V. All rights reserved.
http://dx.doi.org/10.1016/j.physe.2012.03.018

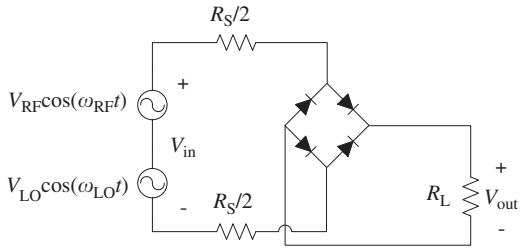

Fig. 1. Circuit diagram of full-wave rectifier which may be used as a switching mixer to mix RF and local oscillator (LO) signals. The output signal, V_{out}, is taken across the load resistance, R_L, and the resistance of the source is R_S.

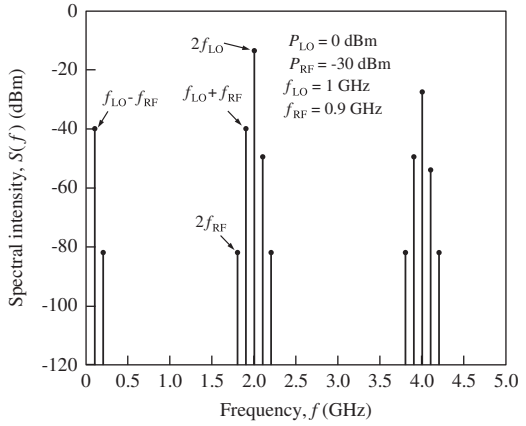

Fig. 2. Spectral intensity of V_{out} of the switching mixer shown in Fig. 1 simulated using LTSPICE. Although mixing has been accomplished, many spurious harmonics are produced. The IF output intensity is -40 dB m for a mixer power gain of -10 dB, and the intensity at frequency $f=2f_{IF}$ is -82 dB m. Simulation parameters are LO power $P_{LO}=0$ dB m and frequency $f_{LO}=1$ GHz, RF power $P_{RF}=-30$ dB m and frequency $f_{RF}=900$ MHz, source resistance $R_S=50\,\Omega$, and load resistance $R_L=50\,\Omega$.

where $V_{in}(t)=V_{LO}\sin(\omega_{LO}t)+V_{RF}\sin(\omega_{RF}t)$ is the total input voltage. Typically the received RF signal is weak and a strong LO is required to drive the diodes. If $V_{LO}\gg V_{RF}$

$$V_{out}(t)\approx\frac{R_L}{R_S+R_L}(V_{LO}\sin(\omega_{LO}t)\,\mathrm{sgn}(\sin(\omega_{LO}t))+V_{RF}\sin(\omega_{RF}t)\,\mathrm{sgn}(\sin(\omega_{LO}t))). \quad (2)$$

Mixing of RF and LO signals occurs through the second term in this expression. Expanding the sign function in terms of its Fourier series

$$\mathrm{sgn}(\sin(\omega_{LO}t))=\frac{4}{\pi}\sum_{n=0}^{\infty}\frac{1}{2n+1}\sin((2n+1)\omega_{LO}t) \quad (3)$$

shows that an infinite set of harmonics are introduced into the output of the mixer. Presence of high-order harmonics requires filtering of the output signal.

The $n=0$ term in Eq. (3)

$$\frac{1}{2}\frac{4}{\pi}V_{RF}\sin(\omega_{LO}t)\sin(\omega_{RF}t) \quad (4)$$

mixes the fundamental LO frequency with f_{RF} to yield

$$V_{IF}(t)=\frac{V_{RF}}{\pi}\cos((\omega_{LO}-\omega_{RF})t). \quad (5)$$

In these expressions the factor of $\frac{1}{2}$ results from setting $R_S=R_L$ for maximum power gain. The power gain of the switching mixer is $1/\pi^2\approx-10$ dB and is independent of V_{LO}.

The spectral intensity of the switching mixer output simulated using LTSPICE, assuming *ideal* switching, is shown in Fig. 2 for LO power $P_{LO}=0$ dB m (1 mW) and frequency $f_{LO}=1$ GHz, RF power $P_{RF}=-30$ dB m (1 μW) and frequency $f_{RF}=900$ MHz, source resistance $R_S=50\,\Omega$, and load resistance $R_L=50\,\Omega$. In this configuration the power contained in the IF is -40 dB m, for a simulated -10 dB power gain. Spurious harmonics produced include even-order LO terms and harmonics at frequencies $(2n+1)f_{LO}\pm f_{RF}$ from Eq. (2), as well as additional terms due to ideal mixing. The fourth order mixing term at frequency $f=2f_{IF}=200$ MHz, containing -82 dB m of power, limits the dynamic range of the switching mixer. Reduction of this harmonic by an additional 48 dB without reducing the power gain of the mixing term would require an eight pole filter, adding complexity to receiver design [3,4].

3. Improved performance of switching mixer with a customized nonlinear diode

Decreasing the spectral intensity of spurious harmonics reduces filtering requirements necessary to achieve a desired large dynamic range. Spurious harmonics can be reduced by adding a nonlinearity such as squaring the output of the switching mixer. Consider the output signal $V_{LO}\sin(\omega_{LO}t)\,\mathrm{sgn}(\sin(\omega_{LO}t))$. Fig. 3(a) shows the effects of squaring this signal in the time-domain. The square-law transfer characteristic converts a rectified sine wave into a pure sine wave by reshaping features in the signal such as discontinuities in the derivative at $V_{bias}=0$ V.

Fig. 3(b) shows these effects in the frequency domain. The spectral intensity of a square wave signal is indicated as dashed

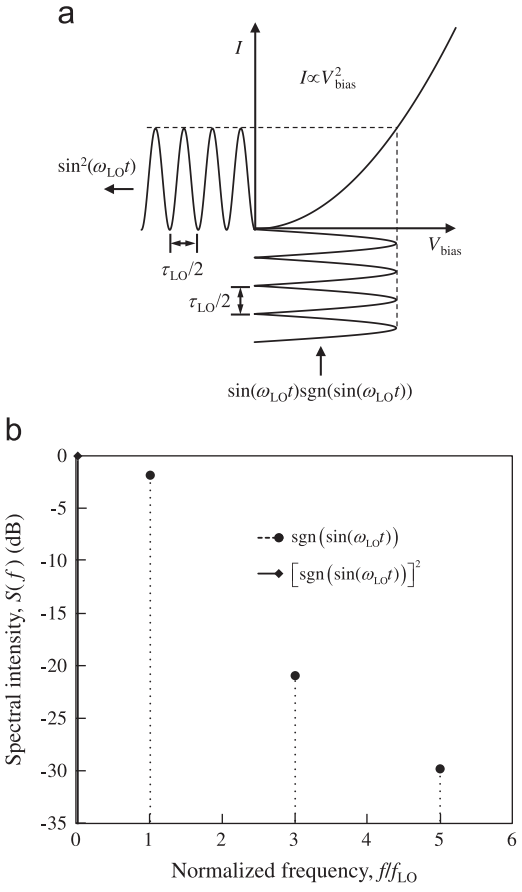

Fig. 3. (a) Diagram showing that a rectified sinusoidal input to a perfect square-law device yields a pure sine wave. (b) Frequency components of a sign function and the square of a sign function. The square-law transfer characteristics redistributes power in an infinite set of harmonics, filtering all frequencies except $f=0$ Hz.

lines in the figure. A square-law transfer characteristic mixes these frequencies such that all harmonics are canceled and power is contained in only the zero frequency term, effectively filtering the harmonics. Thus, a component designed to square the output of the mixer may be able to filter spurious harmonics in the output signal.

As a check we square the output of the ideal switching mixer, Eq. (1). Setting $R_S = R_L$ for maximum power transfer

$$V_{out}(t) = \frac{1}{4}|V_{in}(t)|^2 = \frac{1}{4}V_{LO}^2 \sin^2(\omega_{LO}t) + \frac{1}{2}V_{LO}V_{RF}\cos(\omega_{LO}t)\cos(\omega_{RF}t) + \frac{1}{4}V_{RF}^2 \sin^2(\omega_{RF}t), \quad (6)$$

having the desired mixing term $V_{IF}(t) = \frac{1}{4}V_{LO}V_{RF}\cos((\omega_{LO}-\omega_{RF})t)$, and only second-order spurious harmonics. Additionally the IF amplitude depends on V_{LO}, allowing for variable mixer gain.

To accomplish the squaring action a customized semiconductor heterostructure tunnel diode is designed and the diode placed in series with the load as shown in Fig. 4(a). The equivalent series circuit of the mixer is shown in Fig. 4(b) to simplify circuit analysis. In Fig. 4(b) the rectifying diodes have been omitted, and their functionality contained in the absolute value of the input voltage. The symbol for a parametrically defined diode, to be defined later, features a "C" for "custom" current–voltage characteristic.

For $V_{out}(t) = I(t)R_L$ to be proportional to $|V_{in}(t)|^2$ as in Eq. (6), it is desired that the current through the series circuit equals

$$I(t) = \alpha|V_{in}(t)|^2, \quad (7)$$

where α is a constant coefficient and I is indicated in Fig. 4. Naively, one may expect a diode featuring a quadratic current–voltage characteristic to satisfy Eq. (7). However, summing voltages around the circuit of Fig. 4(b) yields

$$|V_{in}(t)| - \sqrt{\frac{I(t)}{\alpha}} - I(t)(R_S + R_L) = 0, \quad (8)$$

resulting in current that is not proportional to $|V_{in}(t)|^2$.

To satisfy Eq. (7) we will not use a conventional approach to circuit design in which currently existing (and often active) circuit elements are configured to approximate a desired behavior. Rather, a single diode will be designed featuring a customized

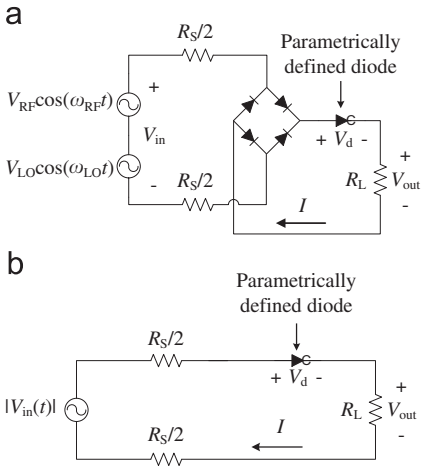

Fig. 4. (a) Circuit diagram of a switching mixer utilizing a parametrically defined diode to eliminate spurious harmonics. (b) Equivalent series circuit of part (a) where the rectifying diodes can be omitted by taking the absolute value of the input voltage. The circuit symbol for the parametrically defined diode features a "C" for "custom" current–voltage characteristic. Inputs to the circuit are RF signal of amplitude V_{RF} and frequency ω_{RF} and LO signal of amplitude V_{LO} and frequency ω_{LO}, and their sum is V_{in}. The source and load resistances are R_S and R_L, respectively.

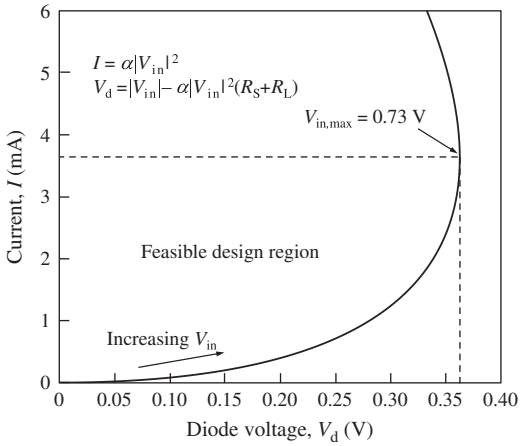

Fig. 5. Parametrically defined diode current–voltage characteristic given by the equations in the figure. A feasible design region is indicated bounded by maximum source voltage, $V_{in,max}$, where the slope $\partial I/\partial V_d = \infty$. Simulation parameters are $\alpha = 6.9$ mA/V^2, source resistance $R_S = 50\ \Omega$, and load resistance $R_L = 50\ \Omega$.

current–voltage characteristic which enables the switching mixer to satisfy Eq. (7).

Supposing a diode can be designed that is capable of satisfying Eq. (7), voltage across the diode is

$$V_d(t) = |V_{in}(t)| - \alpha|V_{in}(t)|^2(R_S + R_L). \quad (9)$$

Thus, the required diode current–voltage characteristic is defined *parametrically* by Eqs. (7) and (9) in terms of V_{in}.

Because the current–voltage characteristic is defined parametrically, the customized diode is not guaranteed to be physically feasible. In fact, we do not know *a priori* if a diode design exists that has the desired nonlinear current–voltage characteristic.

An example current–voltage characteristic is shown in Fig. 5 for $\alpha = 6.5$ mA/V^2, source resistance $R_S = 50\ \Omega$, and load resistance $R_L = 50\ \Omega$. It can be seen that the parametrically defined current–voltage characteristic exhibits multi-valued current, which is potentially unstable, as well as an infinite slope, dI/dV. However, a design is feasible over the voltage range $V_{in} < V_{in,max}$, as indicated in the figure. $V_{in,max}$ is defined as the source voltage at which $(\partial I/\partial V_{in})(\partial V_{in}/\partial V_d) = \infty$, or $\partial V_d/\partial V_{in} = 0$. From Eq. (9)

$$V_{in,max} = \frac{1}{2\alpha(R_S + R_L)}. \quad (10)$$

Designing a tunnel diode capable of achieving the large slope in the current–voltage characteristic near $V_{in} = V_{in,max}$ may be difficult. Designs that can capture this feature may include physical effects such as spectrally narrow electron transmission resonances or may be designed to operate at low temperatures to take advantage of a step-like Fermi–Dirac electron distribution. For our proof-of-principle demonstration we choose to ease the design challenges by optimizing over a smaller range of source voltage at the expense of reducing the IF voltage gain from the theoretical maximum. All designs assume room temperature operation (temperature $T = 300$ K).

Features in the parametrically defined current–voltage characteristic may be explored by comparing the operation of switching mixers with and without the parametrically defined diode. Fig. 6 shows current–voltage characteristics for the series circuit of Fig. 4(b) both with and without the parametrically defined diode, where $R_S = 50\ \Omega$, $R_L = 50\ \Omega$, and $\alpha = 6.9$ mA/V^2.

To ensure that mixer and diode satisfy Eq. (7), the net resistance of the series circuit must be

$$R(V_{in}) = \frac{\partial V_{in}}{\partial I(V_{in})} = \frac{1}{2\alpha V_{in}}. \quad (11)$$

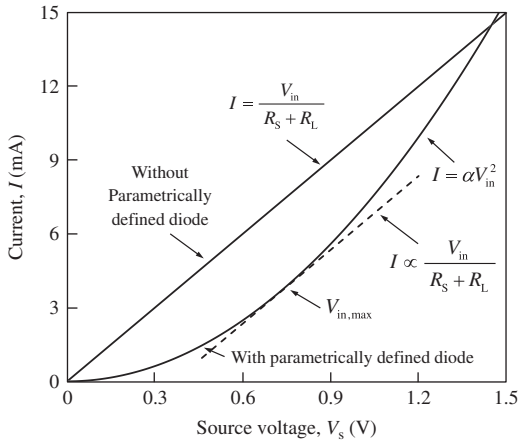

Fig. 6. Comparison of current–voltage characteristics for series circuits with and without the parametrically defined diode. Maximum source voltage, $V_{in,max}$, is defined as the point at which the slope of the parabola matches that of the line. Parameters for the figure are source resistance $R_S = 50\,\Omega$, load resistance $R_L = 50\,\Omega$, and $\alpha = 6.9\ \mathrm{mA/V^2}$, resulting in $V_{in,max} = 0.73$ V.

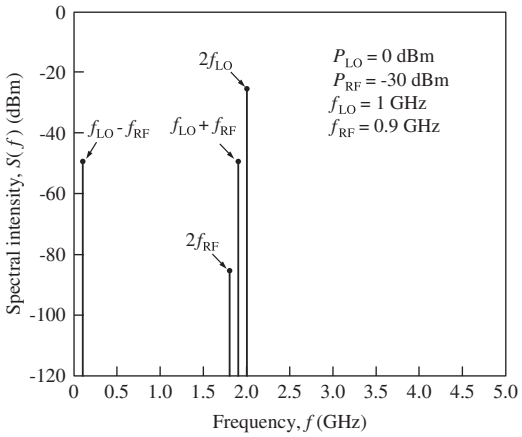

Fig. 7. Spectral intensity of switching mixer output containing parametrically defined diode. The customized current–voltage characteristic of the ideal diode eliminates all spurious harmonics above the second-order terms. The IF power is -49 dB m, for a power gain of -19 dB. Simulation parameters are LO power $P_{LO} = 0$ dB m and frequency $f_{LO} = 1$ GHz, RF power $P_{RF} = -30$ dB m and frequency $f_{RF} = 900$ MHz, source resistance $R_S = 50\,\Omega$, and load resistance $R_L = 50\,\Omega$. The parametrically defined diode is characterized by $\alpha = 6.9\ \mathrm{mA/V^2}$.

Modeling the parametrically defined diode as a voltage dependent resistor requires the diode differential resistance be

$$R_d(V_{in}) = \frac{1}{2\alpha V_{in}} - (R_S + R_L). \tag{12}$$

At input voltage $V_{in} = V_{in,max}$, the slopes of two curves in Fig. 6 are equal, indicating equal values of differential resistance. Since both circuits contain the same R_S and R_L, the differential resistance of the parametrically defined diode must be zero at this value of V_{in}. This physical requirement is satisfied by the infinite slope seen in Fig. 5, while the expression for $V_{in,max}$ may be verified by substituting Eq. (10) into Eq. (12). For input voltages $V_{in} > V_{in,max}$, the diode must have negative differential resistance, while for input voltages $V_{in} < V_{in,max}$, the diode must have positive differential resistance. Both of these features are also present in Fig. 5.

To determine the performance limits of a switching mixer utilizing a parametrically defined diode as illustrated in Fig. 4, it is assumed that $V_{RF} \ll V_{LO}$ such that $V_{LO} \approx V_{in,max}$. Substituting the rectified source voltage

$$|V_{in}(t)| = V_{LO}\sin(\omega_{LO}t)\,\mathrm{sgn}(\sin(\omega_{LO}t)) + V_{RF}\sin(\omega_{RF}t)\,\mathrm{sgn}(\sin(\omega_{LO}t)) \tag{13}$$

into Eq. (7), the IF current is

$$I_{IF} = \alpha V_{LO} V_{RF}\cos((\omega_{LO} - \omega_{RF})t) = \frac{V_{RF}}{2(R_S + R_L)}\cos((\omega_{LO} - \omega_{RF})t), \tag{14}$$

where the expression for Eq. (10) has been substituted for V_{LO}. The average IF power delivered to the load is

$$P_{IF} = \frac{1}{2} I_{IF}^2 R_L = \frac{V_{RF}^2}{8(R_S + R_L)^2} R_L = \frac{1}{16}\frac{V_{RF}^2}{R_S}, \tag{15}$$

where $R_L = R_S$ for maximum power transfer. Since $P_{RF} = V_{RF}^2/2R_S$, maximum power gain is -12 dB (which is about 2 dB less than the power gain of the switching mixer without the parametrically defined diode). Operating with $V_{LO} < V_{in,max}$ reduces power gain.

The output power of a switching mixer utilizing a parametrically defined diode simulated using LTSPICE is shown in Fig. 7. For comparison with Fig. 2, the mixers in both figures use identical simulation parameters. The parametrically defined diode has reduced spurious harmonics to only second-order harmonics and IF power gain is -19 dB. With the ideal parametrically defined diode the lowest frequency spurious harmonic occurs at frequency $f = 2f_{RF}$, easing the requirements of the filter and increasing dynamic range.

4. Voltage gain versus power gain

With power gain of -19 dB, reduction of the harmonics has come at the expense of a 9 dB decrease in power gain. However, it is often the case that a mixer is followed by an amplifier featuring a high input impedance. In this case the *voltage gain* of a mixer is a more suitable figure of merit.

For the two mixers considered, the voltage gain is

$$A_v = \frac{2}{\pi}\frac{R_L}{R_L + R_S}, \tag{16}$$

without the parametrically defined diode and

$$A_v = \tfrac{1}{2}\alpha V_{LO} R_L, \tag{17}$$

with the parametrically defined diode. Substituting $V_{in,max}$ for V_{LO}, the maximum voltage gain with the parametrically defined diode is

$$A_{v,max} = \frac{1}{2}\frac{R_L}{R_L + R_S}. \tag{18}$$

In the following, it will be assumed that the load resistance is $R_L = 600\,\Omega$, and the input power is referred to source resistance of $R_S = 50\,\Omega$. With these values the switching mixer *without* a parametrically defined diode features a voltage gain of -4.6 dB, the maximum voltage gain *with* the parametrically defined diode is -6.7 dB. (For comparison, the voltage gain of the mixer in Fig. 7 is -14.5 dB.)

Fig. 8 shows comparison of the ideal switching mixer voltage gain with $R_L = 600\,\Omega$ with and without the parametrically defined diode in the circuit. As expected, without the parametrically defined diode the gain is constant and with the diode the gain is linearly proportional to V_{LO} with a maximum of -6 dB. In this ideal case elimination of the spurious harmonic at frequency $f = 2f_{IF}$ is achieved, with the spectral intensity of this component at the noise floor < -180 dB V.

5. Optimal design of a parametrically defined diode

To realize a diode defined parametrically by Eqs. (7) and (9), a semiconductor heterostructure tunnel diode is designed using principles of optimal design. This type of device has been chosen

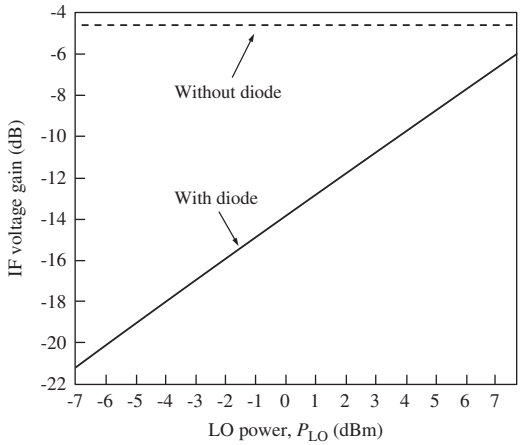

Fig. 8. Ideal IF voltage gain for switching mixer without (dashed) and with (solid) parametrically defined diode. Simulation parameters are $P_{RF} = -30$ dB V (-43 dB V), $R_L = 600\ \Omega$, $R_S = 50\ \Omega$, and $\alpha = 6.9$ mA/V^2.

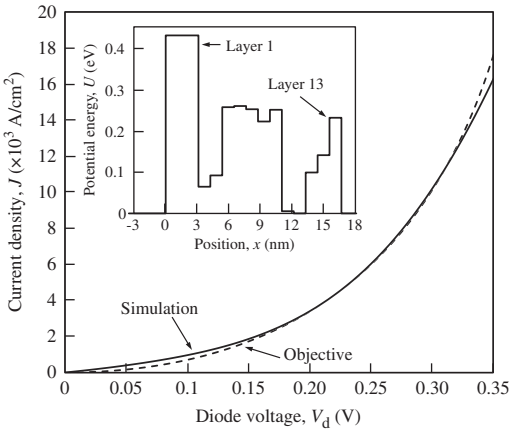

Fig. 9. Simulated (solid curve) current density through a $Al_\xi Ga_{1-\xi}As$ heterostructure tunnel barrier diode optimized for use in a switching mixer. Shown in the inset is the conduction band potential profile for the device. The conduction band offset for each layer is given in Table 1. Simulation parameters are temperature $T = 300$ K, electron effective mass $m = 0.07 \times m_0$, n-type doping concentration $n = 1 \times 10^{18}$ cm^{-3}. The objective function (dashed curve) is characterized by $\alpha = 1$ mA/V^2 and $R_L + R_S = 650\ \Omega$.

for optimization because the ability to manufacture semiconductor layers with atomic precision enables high levels of control over diode current–voltage characteristics. By varying material composition, conduction band potential offsets can be used to manipulate electron tunneling probabilities and electron transmission resonances. We use methods previously developed to design a tunnel diode with linear current–voltage characteristics and dynamic range of up to 65 dB over a peak-to-peak voltage swing of 0.4 V at room temperature [1].

The chosen device structure for optimization consists of an $Al_{0.5}Ga_{0.5}As$ layer of thickness L_0, having a potential energy offset to GaAs of 0.43 eV [5], followed by N $Al_\xi Ga_{1-\xi}As$ layers of thickness $L_\delta = 4 \times \delta$, where $\xi \le 0.35$ (see inset of Fig. 9). At temperature $T = 300$ K a monolayer of (1 0 0)-oriented GaAs is $\delta = 0.2827$ nm thick. In this configuration the $Al_{0.5}Ga_{0.5}As$ layer serves as the primary current-limiter while the $Al_\xi Ga_{1-\xi}As$ layers fine-tune features of the current–voltage characteristic. The GaAs contacts are n-type doped with an electron concentration of $n = 1 \times 10^{18}$ cm.

Current density is calculated using the Tsu–Esaki formula [6], with the potential solved self-consistently between the Schrödinger and Poisson equations. A predictor–corrector scheme [7] is used to solve the Poisson equation, in which a relative permittivity of $\epsilon_r = 13.2 - 2.1 \times \xi$ is assumed [8]. To prevent depletion of the emitter contact in the absence of scattering a drifted Fermi distribution is used [9]. Inelastic scattering into accumulation region quasi-bound states is necessary for generating charge within this region. We assume these bound states to be in thermal equilibrium with the contact electrode [10].

For simplicity we use a conduction band effective electron mass $m = 0.07 \times m_0$, where m_0 is the bare electron mass, in all heterostructure layers. We note that our model captures the essential physics of electron transport through a few nm of $Al_\xi Ga_{1-\xi}As$ heterostructure material. Attempts to include inelastic scattering mechanisms [11] and other details such as conduction band non-parabolicity [12] when total thickness of the active region is less than λ_{in} can add significantly to the complexity of the model. More complex models introduce new ways in which current can flow through the device. However, so long as the change in current is slowly varying with voltage, it should be controllable by adjusting the conduction band potential profile of the active region and hence have little effect on the feasibility of the objective.

Optimization parameters are $Al_{0.5}Ga_{0.5}As$ layer thickness, L_0, and the set of $Al_\xi Ga_{1-\xi}As$ conduction band offsets $\{U_j\}$, where the potential energy of the jth $Al_\xi Ga_{1-\xi}As$ layer is $U_j = 0.8355 \times \xi$ eV. As a measure of the optimality of a given design, the cost function is defined as

$$C = \sum_{i=1}^{v} (J_{obj}(V^i_{bias}) - J_{sim}(V^i_{bias}, p))^2, \tag{19}$$

where design parameters L_0 and $\{U_j\}$ are contained in vector p. Eq. (19) is a least squares measure of the difference between the simulated current density, J_{sim}, and the objective function, J_{obj}. Other choices of measure may be used. The optimization range for the voltage bias is $0 \le V_{bias} \le 0.29$ V, which is 75% of V_d when the input voltage is $V_{in} = V_{in,max}$. Physical constraints are $\xi < 0.42$ ($U_j < 0.35$ eV) and $L_0 = n \times \delta$, where n is a positive integer.

The *fmincon* program available in the optimization toolbox of MATLAB is used to minimize Eq. (19) starting from an initial set of $\{U_j\}$ and L_0. This program uses the Newton–Raphson method to find a locally optimum potential profile and the partial derivatives $\partial C/\partial U_j$ and $\partial C/\partial L_0$ are calculated using the numerically efficient adjoint method [13,14].

The characteristics of a heterostructure tunnel diode optimized for use in a switching mixer is shown in Fig. 9. The diode features $N = 12$ $Al_\xi Ga_{1-\xi}As$ layers, each of thickness $L_\delta = 4 \times \delta$, an $Al_{0.5}Ga_{0.5}As$ layer thickness $L_0 = 11 \times \delta$, and n-type doping concentration $n = 1 \times 10^{18}$ cm^{-3}. Conduction band offsets relative to the GaAs contacts for each layer of the device are given in Table 1. The objective function is characterized by $\alpha = 1$ mA/V^2 and $R_L + R_S = 650\ \Omega$, and the cross-sectional area of the diode is $A = 1.65\ \mu m^2$.

The inset in Fig. 9 is the conduction band-edge potential profile for the device. Features in this potential profile, such as the two potential wells, are selected by the optimization algorithm to control electron resonances that contribute to current. This control mechanism is effective so long as resonance spectral width, $\Gamma_r = \hbar/\tau_r$, has a characteristic time, τ_r, very much smaller than τ_{in}, the inelastic scattering time associated with λ_{in}.

Electron transmission resonances most significantly enhance electron transmission probability when their energies are near those of occupied electron states. The majority of these occupied electron states reside below the chemical potential $\mu = 39$ meV. The potential well at position $x = 12$ nm contributes to lower energy resonances more than those of the potential well at position $x = 4$ nm, which has a higher potential energy offset

Table 1
Conduction band (CB) offsets relative to GaAs contacts for each layer of the optimized, parametrically defined diode shown in Fig. 9.

Layer	CB offset (eV)
1	0.430
2	0.064
3	0.092
4	0.257
5	0.259
6	0.252
7	0.222
8	0.250
9	0.005
10	0
11	0.099
12	0.141
13	0.231

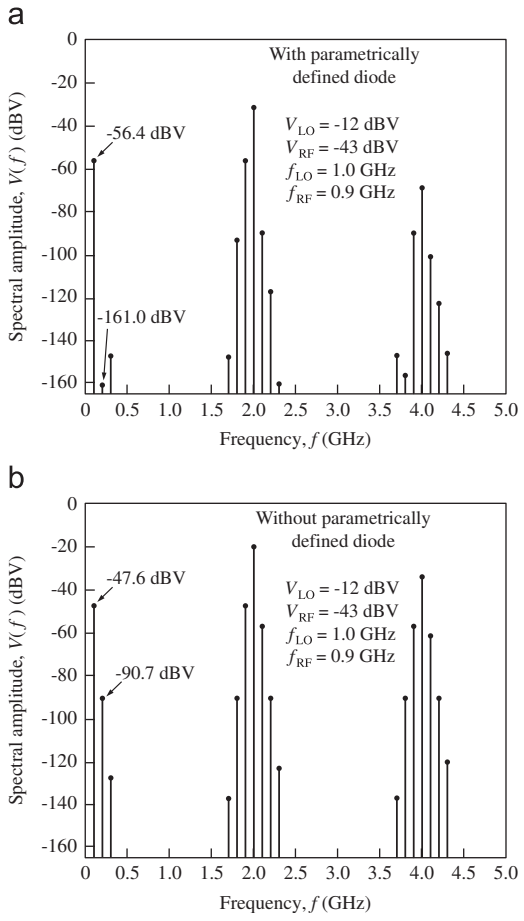

Fig. 10. (a) Spectral intensity of the output of a switching mixer utilizing the optimized parametrically defined diode of Fig. 9. The IF voltage gain for this mixer is −13.4 dB and the amplitude of the fourth order harmonic at frequency $f=2f_{IF}$ is −161.0 dB V. (b) Spectral intensity of the output of a switching mixer without the parametrically defined diode. The IF voltage gain for this mixer is −4.6 dB and the fourth order harmonic at frequency $f=2f_{IF}$ is −90.7 dB V. Simulation parameters are LO power $P_{LO}=1$ dB m (−12 dB V) and frequency $f_{LO}=1$ GHz, RF power $P_{RF}=-30$ dB m (−43 dB V), frequency $f_{RF}=900$ MHz, source resistance $R_S=50\,\Omega$, and load resistance $R_L=600\,\Omega$.

relative to the GaAs contacts. Thus, as V_d lowers the potential of the right-hand contact, the lower energy resonances of the right-hand potential well will overlap the occupied electron states first, controlling current at low voltage bias. The resonances of the left-hand potential well overlap the occupied electron states at higher V_d, controlling current at higher voltage bias.

LTSPICE simulations of the output spectral amplitude for a switching mixer utilizing the optimized diode is shown in Fig. 10(a). Fig. 10(b) shows the output spectral amplitude of the switching mixer *without* the parametrically defined diode. Although non-idealities have introduced additional harmonics compared to the ideal case depicted in Fig. 7, Fig. 10(a) shows that many harmonics produced by the switching action remain suppressed. In particular, the −161.0 dB V amplitude of the $f=2f_{IF}$ harmonic is 70.3 dB V less than that produced by the switching mixer, increasing dynamic range by 61.5 dB. The IF voltage gain with the parametrically defined diode is −13.4 dB V, indicating an 8.8 dB loss in mixer gain for increased dynamic range.

6. Non-idealities in parametrically defined diode

Filtering of spurious harmonics by the parametrically defined diode may only occur within the finite frequency response of the device. The parametrically defined diode is modeled as a resistor in series with the parallel combination of a current source and capacitor. Approximating the GaAs contacts separated by a

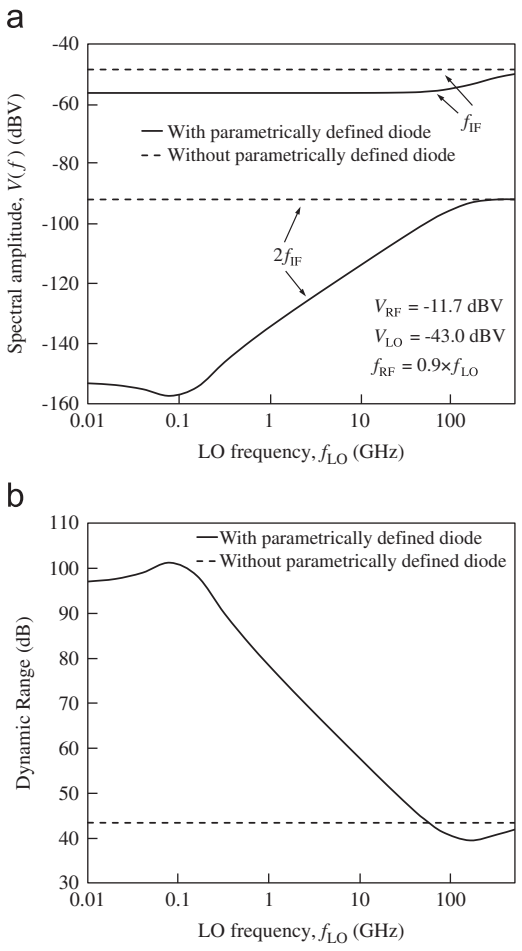

Fig. 11. (a) Spectral intensity of f_{IF} and $2f_{IF}$ harmonics of non-ideal switching mixers with and without the optimized parametrically defined diode. The parametrically defined diode is assumed to have a parasitic capacitance of $C=12$ fF and a contact resistance of 2 Ω. (b) Dynamic range for curves of part (a), showing that greater than 57 dB improvement is possible with the parametrically defined diode. Simulation parameters are LO power $P_{LO}=1.33$ dB m, RF power $P_{RF}=-30$ dB m and frequency $f_{RF}=0.9\times f_{LO}$, source resistance $R_S=50\,\Omega$, and load resistance $R_L=600\,\Omega$.

16.68 nm thick active region as a parallel plate capacitor, the parasitic capacitance is $C=12$ fF. Ohmic loss within the contacts is modeled by a 2 Ω resistor. In addition to diode parasitics, a finite rise time for switching of $\tau = 0.35/f_{LO}$ is included in simulations.

The performance of non-ideal switching mixers with and without the optimized parametrically defined diode are shown in Fig. 11 for LO power $P_{LO} = 1.33$ dB m (-12 dB V), RF power $P_{RF} = -30$ dB m (-43 dB V), RF frequency $f_{RF} = 0.9 \times f_{LO}$, source resistance $R_S = 50\,\Omega$, and load resistance $R_L = 600\,\Omega$. This LO power has been chosen because of enhanced suppression of the $2f_{IF}$ harmonic by the optimized diode at this power. With increasing frequency the impedance of the capacitor decreases, shorting the parametrically defined diode such that the mixer approaches an unmodified switching mixer. The change may be characterized by the cutoff frequency due to the RC delay within the circuit. The 12 fF parasitic capacitance of the diode in series with 652 Ω of resistance yields a time constant of $\tau = 7.82$ ps and cutoff frequency $f_c = 20.34$ GHz. This is approximately the frequency at which the voltage gain of the mixer with the parametrically defined diode begins to deviate from its low frequency gain.

The parametrically defined diode is shown to enhance dynamic range between f_{IF} and $2f_{IF}$ by better than 15 dB for LO frequencies up to $f_{LO} = 10$ GHz. Fig. 11(b) shows the dynamic range for the curves in Fig. 11(a). Dynamic range improvement of greater than 57 dB is possible at a mixer voltage gain of -13.3 dB.

7. Summary

Nonlinear current–voltage characteristics suitable for analog processing of electronic signals may be designed using nano-scale semiconductor heterostructures. Elastic electron scattering from a conduction band potential profile defined by atomic layer control of semiconductor composition can be used to create desired nonlinear current–voltage characteristics in a tunnel diode. We have successfully demonstrated that the nonlinear device behavior needed to dramatically improve RF mixer performance is physically possible in an $Al_\xi Ga_{1-\xi}As$ heterostructure tunnel diode.

A combination of parametrically defined nonlinear circuit elements and optimal design to discover nano-scale configurations that behave as desired has the potential to enhance the functionality of nano-electronic circuits and may enable access to previously unavailable circuit behavior. However, beyond the proof-of-principle demonstrated here, the generality of the approach, in particular the constraints on achievable nonlinear current–voltage behavior imposed by the physics of nonequilibrium electron transport in small ($\ll \lambda_{in}$) nano-scale active regions, remains to be explored.

Acknowledgments

This research is partially supported by the ARO MURI Grant W911NF-11-1-0268.

References

[1] K.C. Magruder, A.F.J. Levi, Physica E 44 (2011) 322.
[2] T.H. Lee, The Design of CMOS Radio-Frequency Integrated Circuits, Cambridge University Press, New York, 1998.
[3] D. Huang, S. Kao, Y. Pang, A WiMAX receiver with variable bandwidth of 2.5–20 MHz and 93 dB dynamic gain range in 0.13-μm CMOS process, in: IEEE Radio Frequency Integrated Circuits Symposium, 2007, p. 369.
[4] T. Tikka, J. Ryynänen, K. Halonen, Multiband receiver for base-station applications, in: IEEE Radio and Wireless Symposium, 2008, p. 871.
[5] I. Vurgaftman, J.R. Meyer, L.R. Ram-Mohan, Journal of Applied Physics 89 (2001) 5815.
[6] R. Tsu, L. Esaki, Applied Physics Letters 22 (1973).
[7] A. Trellakis, T. Galick, A. Pacelli, U. Ravaioli, Journal of Applied Physics 81 (1997) 7880.
[8] S. Adachi, Journal of Applied Physics 58 (1985) R1.
[9] W. Pötz, Journal of Applied Physics 66 (1989) 2458.
[10] T. Fiig, A.P. Jauho, Applied Physics Letters 59 (1991) 2245.
[11] P. Roblin, W. Liou, Physical Review B 47 (1993) 2146.
[12] R.C. Bowen, G. Klimeck, R.K. Lake, W.R. Frensley, T. Moise, Journal of Applied Physics 81 (1997) 3207.
[13] K.C. Magruder, P. Seliger, A.F.J. Levi, Optimal Device Design, Cambridge University Press, New York, 2010.
[14] A.F.J. Levi, I.G. Rosen, SIAM Journal on Control and Optimization 48 (2010) 3191.